Theoretical Aircraft Overflight Sound Peak Shape

Introduction and Overview

This report summarizes work to characterize an analytical model of aircraft overflight noise peak shapes which matches well with real-world observations of peak shapes from the field. The underlying goal is to be able to use this model to investigate mathematically the behavior of various noise level metrics, with emphasis on the Federal Aviation Administration's (FAA's) customary metric for aircraft noise, the Day-Night Average Sound Level (DNL) — the logarithm of the weighted daily average sound energy.

It is shown that overflight peaks for a typical track have a simple functional form in which the amplitude of the peak is coupled to its width. The more distant an aircraft overflight is, the smaller the peak amplitude, but the greater the peak width. Rather than falling off according to $1/r^2$ (r is the distance from the aircraft to the observer), as with most point source wave phenomena metrics, the integrated sound energy falling on an observer for a given peak falls off only as $1/r$. This has ramifications for the behavior of the DNL metric, making it less sensitive to changes in aircraft altitude and path. (The relationship to DNL measurements is discussed in another paper – see this link.)

The presentation is somewhat mathematical in nature, but is illustrated with many practical examples and graphs. The organization of what follows is summarized below:

Relevant Physics and Mathematics

1) First Order Considerations

To first order, we can compute the profile of an aircraft overflight noise peak based on the geometry of the overflight and the simple physics of sound attenuation with distance for a point source ($\propto 1/r^2$). Assume that an aircraft is flying relative to an observer in a straight path with constant velocity, **v**, at a horizontal ground distance, **d**, and a constant altitude, **h** (see Figure 1). Also assume for now that any atmospheric attenuation of the sound is negligible relative to the $1/r^2$ fall off in intensity with distance; that there are no complications of anisotropy (e.g., engines louder in the rear than in front); that refractive properties of the air between the aircraft and the observer are negligible, and that the finite velocity of sound can be ignored for the time being (i.e., the observer hears the noise without delay).

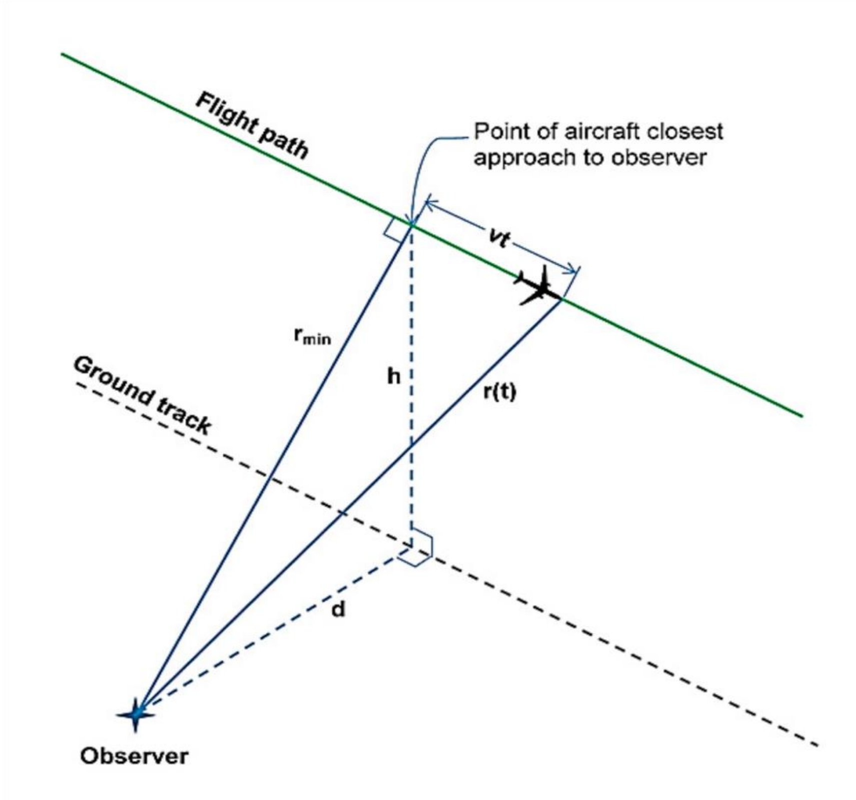

Figure 1: Diagram of aircraft overflight geometry relative to a ground observer.

At time, **t=0**, let the aircraft be at the point of closest approach to the observer (distance $\mathbf{r_{min}}$). Let the aircraft emit sound with an intensity, $\mathbf{I_0}$ (energy per second). Then the sound intensity heard by the observer, $\mathbf{I_{obs}}$, is:

$$\mathbf{I_{obs}(t) \propto \frac{I_0}{r^2(t)}} \qquad (1)$$

where $$\mathbf{r^2(t) = r_{min}^2 + (vt)^2} \qquad (2)$$

and $$\mathbf{r_{min}^2 = d^2 + h^2} \qquad (3)$$

Then if $\mathbf{I_{obs}}$**(max)** is the sound intensity heard by the observer at the point of closest approach of the aircraft,

$$\mathbf{I_{obs}(max) \propto \frac{I_0}{r_{min}^2} = \frac{I_0}{d^2+h^2}} \qquad (4)$$

From equations 1 — 4, we see that the general aircraft noise peak takes the form,

$$\mathbf{I_{obs}(t) \propto \frac{I_{obs}(max)}{[1+\left(\frac{vt}{r_{min}}\right)^2]}} \qquad (5)$$

Note that the "proportional" symbol, ∝ is used in Equations 1, 4, and 3 because there may be some atmospheric attenuation or refraction of the intrinsic sound level, $\mathbf{I_0}$, between the aircraft and observer over and above the $\mathbf{1/r^2}$ falloff.

This function (known as a Lorentzian function familiar in physics and as a Cauchy distribution in probability theory), as shown in the example in Figure 2, has the property that the half-amplitude width of the peak is given by,

$\mathbf{vt_{1/2} = r_{min}}$ or

$$\mathbf{t}_{½} = \frac{\mathbf{r}_{\mathbf{min}}}{\mathbf{v}} = \frac{\sqrt{\mathbf{d}^2+\mathbf{h}^2}}{\mathbf{v}} \qquad (6)$$

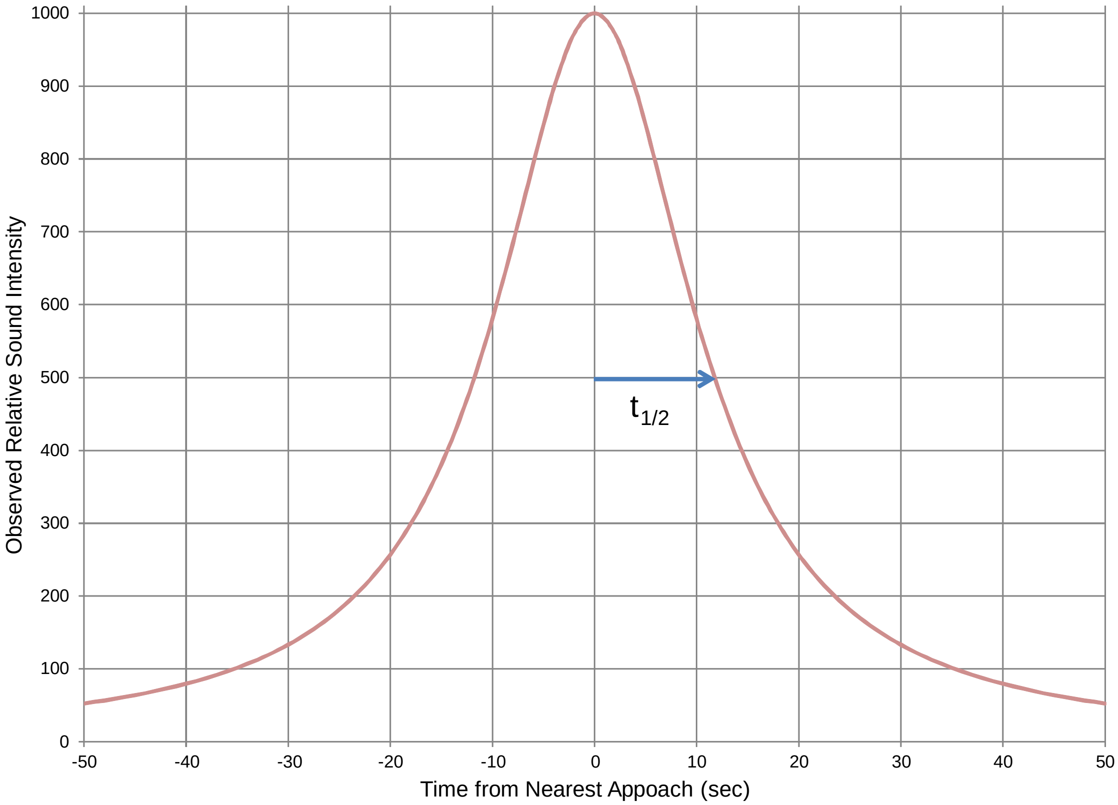

Figure 2: Typical Lorentzian aircraft noise peak shape. The peak shown corresponds to a commercial aircraft flying at 4000 ft and with a velocity of 340 ft/sec (200 knots). The amplitude is set to 1000 intensity units for plotting convenience. The half-width is 11.8 sec.

Geometrically, the half width occurs when the line from the observer to the aircraft makes a 45° angle with the line of closest approach and with the flight path to form a 1:1:$\sqrt{2}$ right triangle (see the sketch in Figure 1).

So, for a given aircraft velocity and altitude, such as shown in Figure 2, we ask “How does the observed peak height and width change with the distance of closest approach?” From Equations 4 and 6, it is clear that the loudest and narrowest noise peak occurs when the plane flies directly overhead (i.e., the distance of closest approach, $\mathbf{r}_{\mathbf{min}}$, is the smallest). However, as the distance of closest approach of the aircraft increases — either because of higher altitude, **h**, or greater distance of the ground track from the observer, **d** — two things happen. First, the maximum observed peak amplitude changes by the reciprocal square of the distance to the aircraft (see Equation 4). Second, the peak half-width changes linearly with the distance of closest approach (see Equation 6).

These opposite effects may seem counterintuitive but they are real for observed overflights and have a strong impact on common measures of aircraft overflight noise, such as the FAA’s DNL metric.

To see how these effects play off against each other, consider the examples shown in Figure 3, where typical noise profiles are plotted for different altitudes (3,000 and 4,000 ft) and for various distances from direct overflight. The intensity level is normalized to 1000 for the loudest aircraft peak, flying directly overhead at 3,000 ft. The colored diamond-shaped markers indicate the locations of the half-width points for the respective peaks.

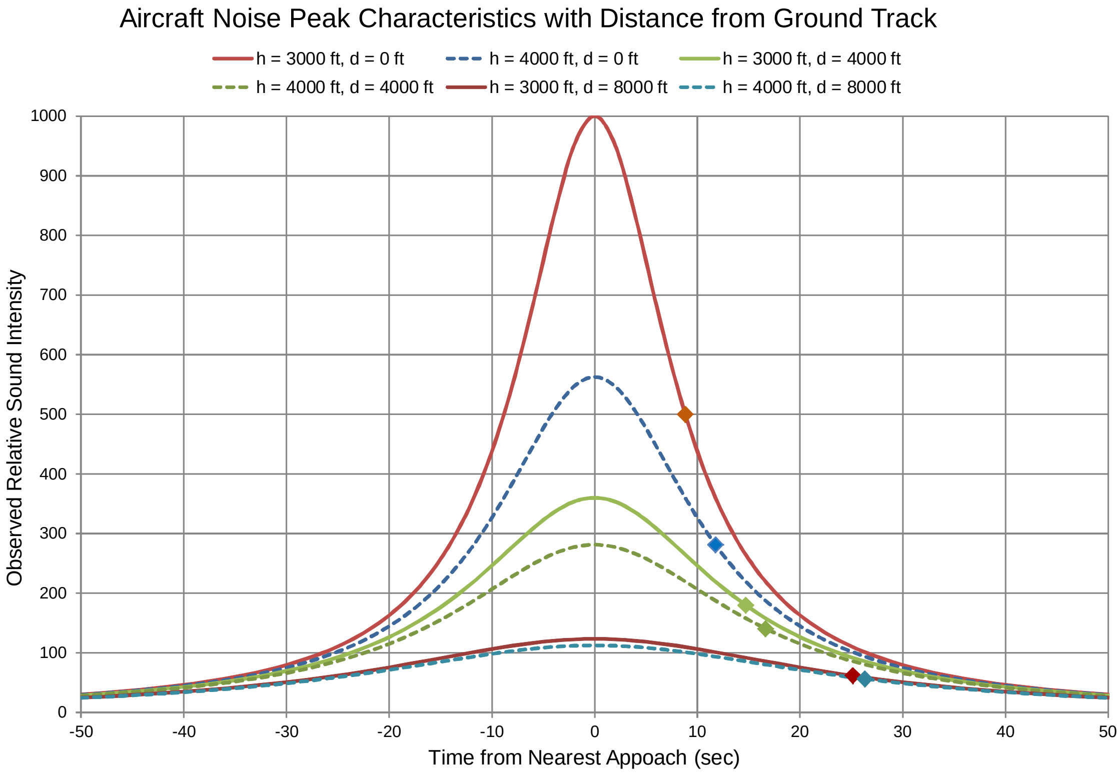

Figure 3: Aircraft overflight noise profiles varying by ground track distance from the observer and altitude. The colored diamond-shaped markers indicate the locations of the half-width points. Note that the peak widths increase with decreasing maximum intensity (i.e., with increasing $\mathbf{r_{min}}$). See Eqns 4 and 6.

The $\mathbf{1/r_{min}^2}$ behavior of the peak maximum is clear — for an altitude increase from 3000 ft to 4000 ft and a lateral distance of 0 ft, the peak maximum drops by nearly 1/2 (i.e., 0.56 which is 3000/4000 squared). At the same time, the peak half-width for this geometry increases by a factor of 1.33, from 8.8 sec to 11.8 sec (i.e., 4000/3000). [Note that the 11.8 second width in Figure 2 shows up again here for the 4000 ft overflight.]

2) Calculating Integrated Sound Energy

Because common measures of noise level are based either on the area under sound intensity curves or on the average of the sound intensity levels over some period of time, it is useful to compute the area, **E**, under the noise intensity curve (see Equation 5) — i.e., the total sound energy in the noise peak. To do this, we note that equation 5 has the form:

$$\mathbf{I_{obs}(t) \propto \frac{A}{1+(\alpha t)^2}}$$ where **A** is $\mathbf{I_{obs}(max)}$ and **α** is $\mathbf{v/r_{min}}$.

Using a convenient table of integrals, we can show that,

$$\mathbf{E} = \int_{-\infty}^{\infty} \mathbf{I_{obs}(t)}\,\mathrm{dt} = \mathbf{A}\int_{-\infty}^{\infty} \frac{\mathbf{1}}{\mathbf{1+(\alpha t)^2}}\,\boldsymbol{dt} = \frac{\mathbf{A}}{\boldsymbol{\alpha}}\,[\mathbf{arctan}(\infty) - \mathbf{arctan}(-\infty)] = \frac{\mathbf{A}\,\boldsymbol{\pi}}{\boldsymbol{\alpha}}$$

and so,

$$\mathbf{E} = \boldsymbol{\pi}\,\frac{\mathbf{I_0}}{\mathbf{r_{min}^2}}\,\frac{\mathbf{r_{min}}}{\mathbf{v}} = \boldsymbol{\pi}\,\frac{\mathbf{I_0}}{\mathbf{v\,r_{min}}} \qquad (7)$$

An interesting point is that whereas the peak maximum varies as $\mathbf{1/r_{min}^2}$, the total energy under the curve (area) varies only more slowly as $\mathbf{1/r_{min}}$. This unusual fact will be important when we consider its implications for the choice of noise metrics and for which measure(s) might be more appropriate to estimate subjective effects of noise.

3) Other Considerations for the Simple Model

Even under the simplifying assumptions in the first order derivation above, two additional influences on the peak shape are important to consider:

1. The velocity of sound is finite and this affects the delay and shape of the noise peak as heard by an observer (as opposed to what is generated at the aircraft). This common phenomenon is called the Doppler effect, which we hear all the time with passing trains or other moving objects that emit sounds.
2. When the aircraft is relatively far from the point of closest approach, the sound must pass through a significantly longer air column so that sound intensity loss by absorption and scattering, over and above the $1/r^2$ factor, cannot be ignored. Typically, these effects are frequency dependent, in that higher frequency sounds are lost in transit more than the lower frequencies. One hears this as an aircraft approaches from a distance and sounds much more like a low frequency rumble than when it is near and more of the full sound spectrum is audible.

a) Velocity-of-Sound (or Doppler) Effects

As the aircraft approaches the point of closest approach, the time of arrival of noise sounds at the observer is compressed and as the aircraft leaves the point of closest approach, the time of arrival of sounds at the observer is stretched out. Using the geometry in Figure 1, the equation describing this effect is simple. If $\mathbf{t_a}$ is the time the sound is generated at the aircraft, $\mathbf{t_{obs}}$ is the time it is heard by the observer on the ground, $\mathbf{r(t_a)}$ is the distance between the observer and the aircraft at time $\mathbf{t_a}$, and $\mathbf{v_s}$ is the velocity of sound, then:

$$t_{obs} = t_a + r(t_a)/v_s \qquad (8)$$

So, for example, if we convert Figure 2 (which was plotted against time at the aircraft, i.e., no delay) into a plot of what the observer on the ground will hear, we get the peak shown in Figure 4. One can see that the peak is delayed by 3.6 sec because of the time it takes the sound to travel from the aircraft to the ground.

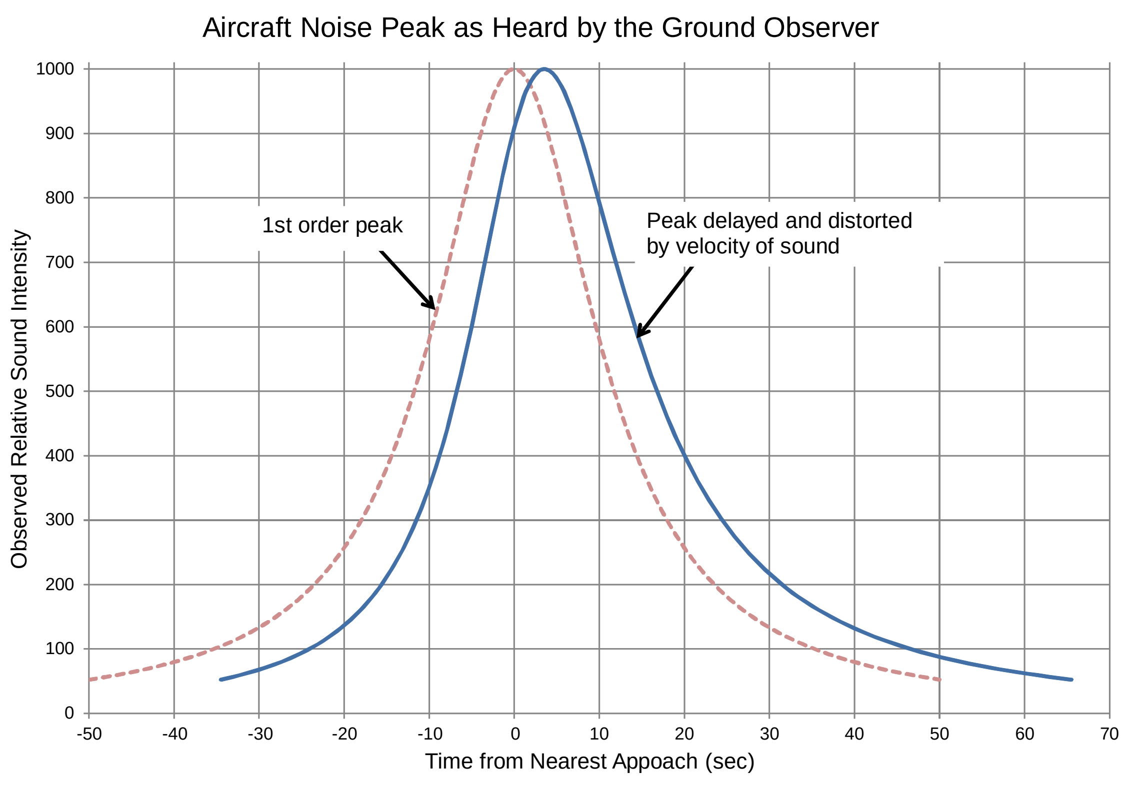

Figure 4: Noise peak shifted by 3.6 seconds because of the finite velocity of sound.

If we then align the arrival time of the observed peak with that of the first order peak, we get Figure 5. Here one can see the shape distortion caused by the velocity of sound — the compression of the leading edge of the peak and the expansion of the trailing edge relative to the peak maximum.

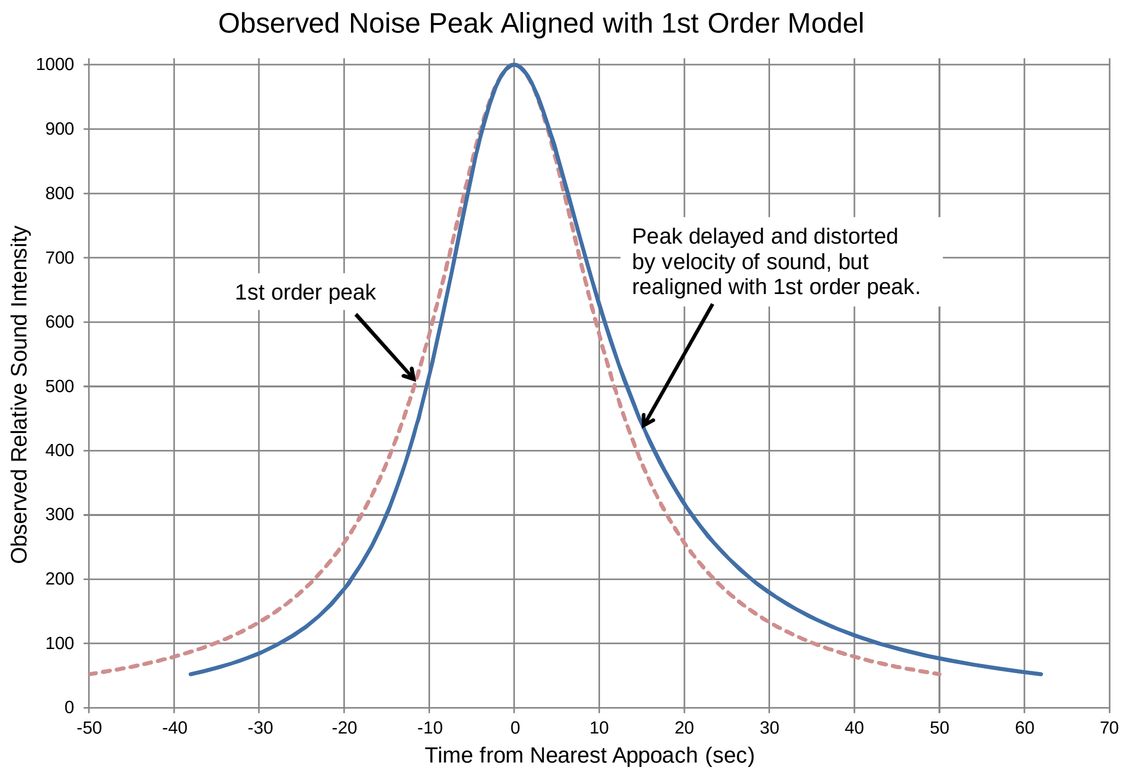

Figure 5: Peak realigned with 1st order peak to see the shape distortion from the finite velocity of sound. Note the compression of the upslope and the dilatation of the downslope of the peak.

b) Atmospheric Loss Effects

The attenuation of the sound by scattering, absorption, and refraction while traveling increasing distances through the air is another important effect on how the observer hears the noise generated by the aircraft. Again a simple model suffices if the attenuation factor is small. Let **I(r)** be the sound intensity at distance **r** along its path (basically following the $1/r^2$ law), let **f** be the attenuation factor per unit distance for sound traveling in air, let $\mathbf{I_{obs}(r)}$ be the intensity heard at the observer without attenuation, and let $\mathbf{I_{obs}^{attenuated}}$ be the attenuated sound heard by the observer. Then we can write the (simplified) differential equation:

$$\mathbf{dI \approx -f\, I\, dr}$$

Then, integrating:

$\mathbf{\ln I \approx -f\, r + C}$ where C is an arbitrary constant.

Then, setting boundary conditions,

$$\mathbf{I_{obs}^{attenuated}(r) \approx I_{obs}(r)\, e^{-f\,(r-r_{min})}; \quad r > r_{min}} \qquad (9)$$

If we apply this additional adjustment to the peak shown in Figure 5, using an attenuation factor of 0.003% per foot, we get Figure 6. One can see that the sound intensity in the wings of the peak is decreased by an amount that increases with distance.

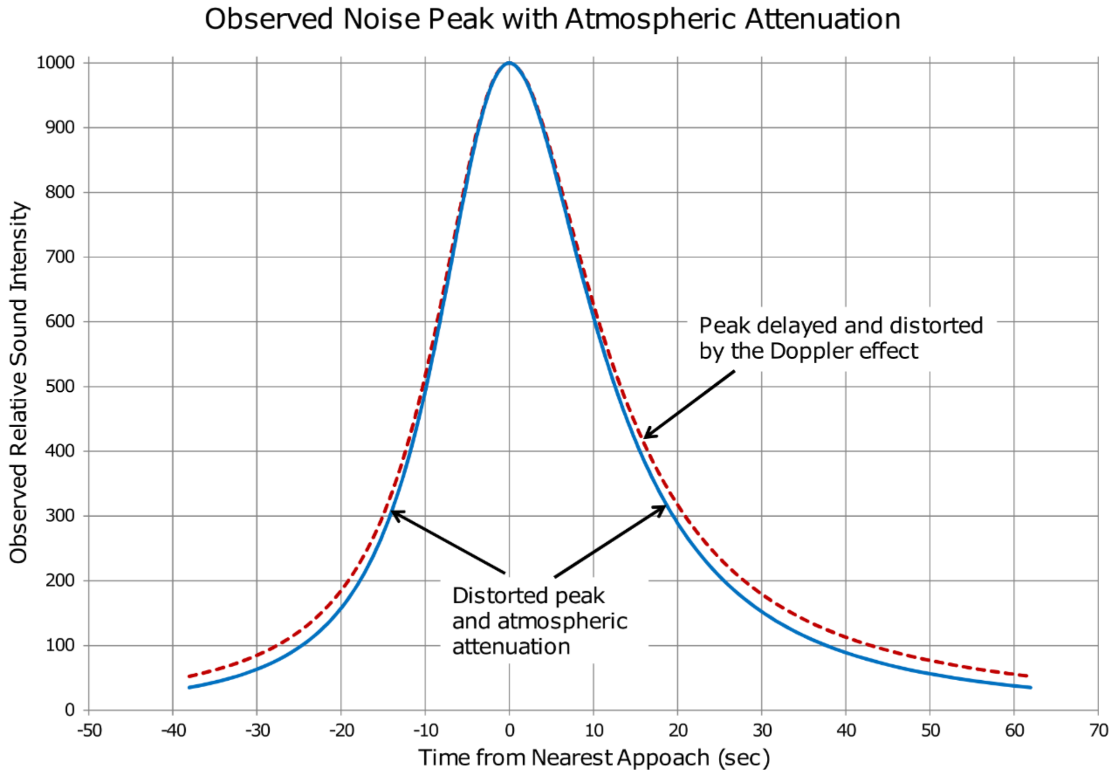

Figure 6: Adjustment of the peak in Figure 5 by applying the correction for atmospheric attenuation from the source.

4) Summary of Parameters in the Simple Model

With this fairly simple model, we can fit actual aircraft overflight sound peak data by adjusting the following parameter set:

1. The maximum observed peak sound intensity, $\mathbf{I_{obs}(max)}$.
2. The values of the aircraft speed, **v**, and its distance of closest approach, $\mathbf{r_{min}}$; actually their ratio, $\mathbf{r_{min}/v}$, suffices to set the basic geometry of the noise peak.
3. The velocity of sound in the air, $\mathbf{v_s}$, depending on weather conditions.
4. The attenuation coefficient, **f**, for sound losses (other than the $\mathbf{1/r^2}$ law) during propagation through the air, again depending on atmospheric conditions.

5) Other Real-World Complexities

Up until now, we have assumed a simplified overflight model: straight-line flight path, constant altitude and distance from the flight path, constant velocity, constant aircraft noise emission, and uniform weather conditions. What happens to the model if the plane is descending to land, is slowing down for an approach, is making a turn to align for an approach, extends flaps or air brakes so it emits more noise, or flies through an inversion or cloud layer? The answer is that the basic physics stays the same but all or some of the model parameters become functions of time. So, for example, if the plane is changing altitude, the parameter **h**, and also the parameter $\mathbf{r_{min}}$, become functions of time. If the plane is making a turn, we either have to approximate its path as a series of line segments or adjust the geometry in Figure 1 to make the path some 3-dimensional arc. This all makes calculating the peak shape, area, etc. in closed form more difficult analytically. Nevertheless, as in the calculus, if we break the path into small enough steps ($\delta t \sim \varepsilon$), the calculation (possibly numerical) follows the same logic as discussed above. Fortunately, major segments of commercial flight paths are fairly straight (passengers don't like to be jostled around), and the formulas above are pretty good approximations.

Some Analysis and Commentary

1) Quality of the Model Fit to Raw Data

A first question is, “How well does the Lorentzian peak profile, described above, approximate what is actually measured in real world noise recordings?” Figure 7 shows two sets of data taken at random from a sound monitor recording collected by the author on August 3, 2015, in north Palo Alto, CA. The first set of plots shows the raw data for a 73.5 dB overflight peak occurring at about 40 minutes past midnight (blue line), with a Lorentzian fit (red line). The second set shows the raw data for a 65 dB peak occurring at about 6:55 AM (green line), with a Lorentzian fit (purple line).

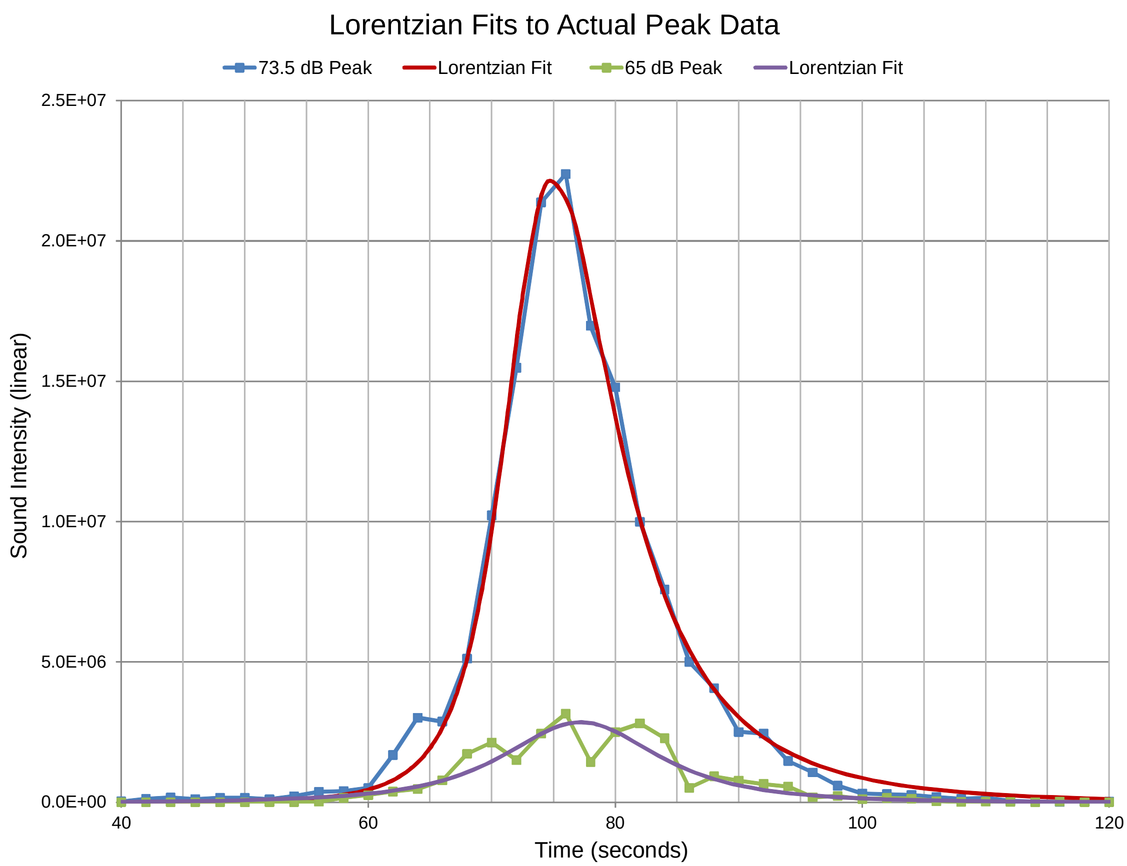

Figure 7: Comparison of raw noise peak data with Lorentzian fits for two overflight events on August 3, 2015, in north Palo Alto, CA.

The parameters were adjusted to optimize the fit and, subjectively, the fits are quite reasonable approximations to the raw data, given the noisy context of the raw data collected, especially for the 65 dB peak. For the 73.5 dB peak, the value of $\mathbf{v/r_{min}}$ is 0.157 and the atmospheric attenuation coefficient is estimated at 0.017% per foot. For the 65 dB peak, the value of $\mathbf{v/r_{min}}$ is 0.114 and the atmospheric attenuation coefficient is about 0.015% per foot. The velocity of sound is assumed to be just over 1100 ft/sec in both cases. If the aircraft producing the peaks were flying at about 500 ft/sec (300 knots), for the 73.5 dB peak, it would be at approximately 3200 ft altitude and for the 65 dB peak at about 4400 ft altitude.

2) Practical Limits of Peak Detection against Background Noise

One more practical measurement issue remains to be noted. Since the aircraft noise is competing with general ambient background noise, the observer can only detect the aircraft noise if it is intense enough so that its sound signature (amplitude, duration, frequency content, etc. corresponding to jet, propeller, or helicopter aircraft) stands out above the background. This means that we must set a detection threshold and measure peak width based on some threshold sound intensity level on the vertical axis of Figure 2. If we arbitrarily choose thresholds of 5%, 10%, and 20% of the loudest aircraft sound intensity under simulated data collection circumstances, i.e., the observed noise for a direct overflight at 4,000 ft and 340 ft/sec (200 knot) velocity, we can plot expected detectable noise peak widths as a function of the aircraft altitude and observer's distance from the ground track (see Figure 3).

The examples in Figure 8 are constructed to show what happens when the aircraft altitude is nearly constant, and the observer's distance from the aircraft ground track (x axis) and the threshold for detectability of the aircraft noise above background are varied. This illustrates a situation such as one might find near a waypoint at which the aircraft altitude is fairly well established but different observers hear the crossing from different distances and background noise settings. Clearly the apparent peak duration varies considerably with distance and threshold.

Of course, variations in aircraft speed, inherent noise intensity generated, and atmospheric transmission and refractive conditions will also affect the perceived noise profile at the observer.

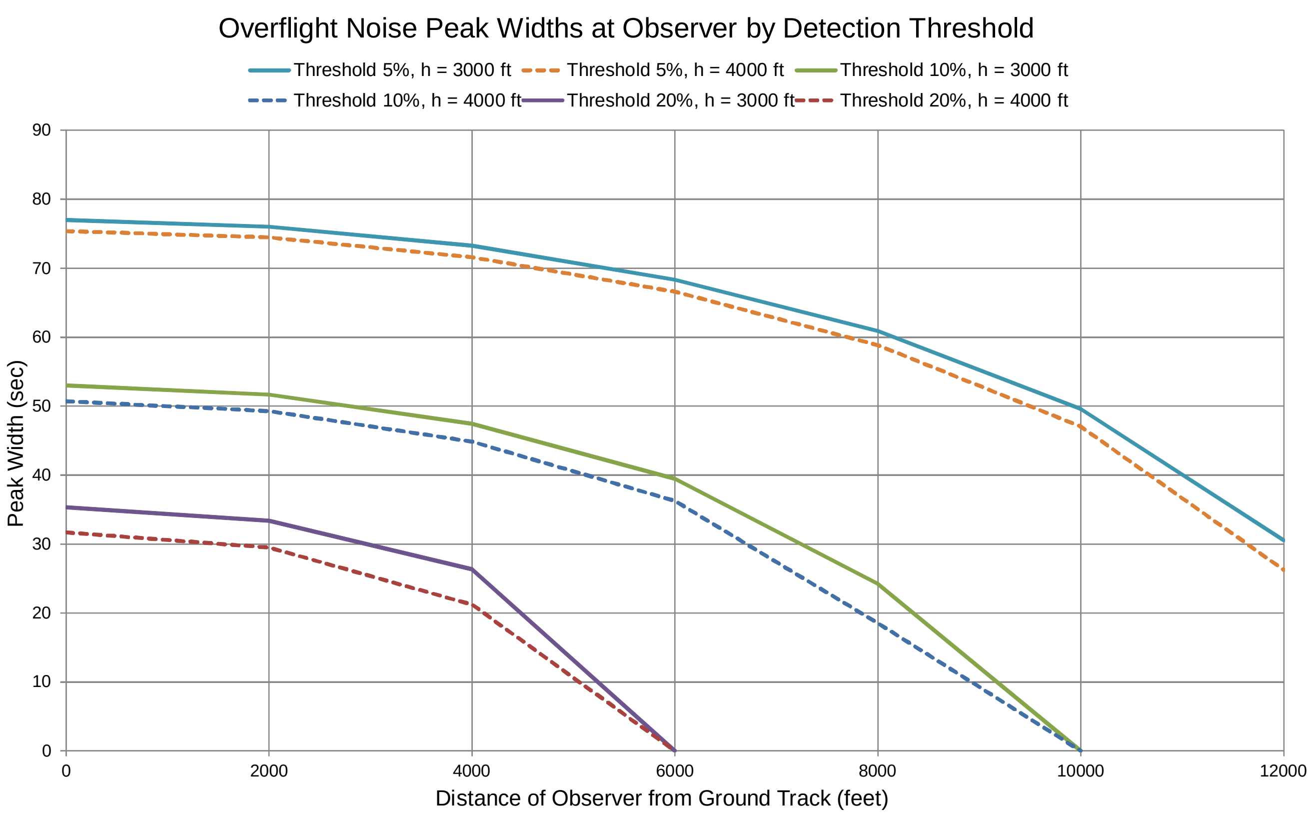

Figure 8: Overflight peak widths vs observer distance from ground track and detection threshold. Aircraft altitude is held relatively fixed.

Peak widths have an effect on the observer through the length of time that daily activities are disrupted by overflight noise. As might be expected, detected durations are largest in relatively quiet background noise periods for which the lower detection thresholds apply. Even though the theoretical peak half-width increases with $\mathbf{r}_{\mathbf{min}}$,(see Equation 6), this effect is dominated by the stronger peak amplitude decrease ~$\mathbf{1/r_{min}^2}$ (see Equation 4) in determining when peak boundaries are detectable. We believe that the peak amplitude factor is more important in determining interference with human activity.